AIP | Chaos
An Interdisciplinary Journal of Nonlinear Science

# A fractal theory based fractional diffusion model used for the fast desorption process of methane in coal

Haina Jiang, Yuanping Cheng, Liang Yuan, Fenghua An, and Kan Jin

Citation: Chaos **23**, 033111 (2013); doi: 10.1063/1.4813597
View online: http://dx.doi.org/10.1063/1.4813597
View Table of Contents: http://chaos.aip.org/resource/1/CHAOEH/v23/i3
Published by the AIP Publishing LLC.

# A fractal theory based fractional diffusion model used for the fast desorption process of methane in coal

Haina Jiang,[1,2] Yuanping Cheng,[1,2,a)] Liang Yuan,[3] Fenghua An,[1,2] and Kan Jin[1,2]
[1]National Engineering Research Center of Coal Gas Control, China University of Mining and Technology, Xuzhou, Jiangsu 221116, China
[2]Faculty of Safety Engineering, China University of Mining and Technology, Xuzhou, Jiangsu 221116, China
[3]National Engineering Research Center of Coal Gas Control, Huainan, Anhui 232000, China

(Received 24 March 2013; accepted 26 June 2013; published online 17 July 2013)

Based on the realistic property of the pore structure in coal, we established a fractal theory based Fractional diffusion model (FFDModel) by introducing the fractal dimension $d_f$ to the Fick's classical model and changing the first-order partial differential equation about time into a $\upsilon$ fractional-order partial differential equation. Then, the solution of the FFDModel was obtained with separation variables technique. In order to verify the correctness of the solution, three coal samples with different rank from China were collected to do the methane desorption experiment of the fast desorption stage. The results indicate that the fractal dimension ($d_f$) of the coking coal is the lowest of the three coal ranks. By comparing the FFDModel with Fick's classical model, we can see that the FFDModel fits better with the three measured samples. © *2013 AIP Publishing LLC*.
[http://dx.doi.org/10.1063/1.4813597]

**This article is prepared in view of the present disadvantages of the Fick's classical model. To describe the natural heterogeneous character of coal, the fractal dimension that can reflect the roughness of the coal surface was introduced to the Fick's classical model and by considering the realistic diffusion in nature, the first-order partial differential equation about time in Fick's classical Model was substituted by a $\upsilon$ fractional-order partial differential equation. Thus, a new fractal theory based Fractional diffusion model (FFDModel) was established. And in order to apply it on the heterogeneous porous materials that universally exist in nature, the solution of the FFDModel was obtained with separating variable method. In order to confirm its validity, we adopt it in the fast desorption process of methane in coal for the first time and found that the FFDModel fits better than the Fick's classical model in the fast desorption stage of methane in coal.**

## I. INTRODUCTION

Recent studies have shown that the pore structure has great effects on gas diffusion in a porous media. Usually, a great variety of diffusion problems in nature, which are referred to as "normal diffusion", are satisfactorily described by Fick's classical model based on the assumption of homogeneous pore structure, and the diffusivity $D_F$ in the model is the unique parameter.[1,2]

However, there are still many cases in which the Fick's classical model fails to capture gas transport in heterogeneous porous media that exhibit fractal characteristics.[3–5] In recent years, intensive analytical and numerical works have been performed to elucidate the anomalous diffusion phenomenon on fractal structures. Much interest has been focused to understanding diffusion processes on such spatially correlated media. Diffusion on fractals exhibits many anomalous features due to the geometrical constraints imposed by the complex structure on the diffusion process. To analysis the effect of complicated pore structure in a porous media on the diffusive kinetics, O'Shaughnessy and Procaccia (1985)[6] obtained a representative fractal model (OP model) based on the introduction of fractal dimension $d_f$ and the equation with which effective diffusivity $D_e$ is a function of $r$ in the form of $D_e = D_0 r^{-\theta}$ (for detail in Appendix), where $D_0$ is the pre-exponential factor, $\theta$ is a structure parameter describing the transport path of the diffusing molecule that is walking in the fractal porous material.[7,8] Wang *et al.* (2009)[9] used the OP model to describe the diffusion of gases in a porous material within the limited volume of a stiff container (LVSC) and found that the OP model would lead to a more realistic description of the diffusion process in a porous material since the calculated results fit better with the experimental curves than the Fick's classical model. Zheng *et al.* (2012)[10] derived a fractal model for gas diffusivity in fractal porous media in the steady state and found that the fractal dimensions and porosity have significant influences on the gas diffusivity, and the effective diffusivity $D_e$ will increases monotonously with the increase of the pore fractal dimension.

The fractal diffusion model is the approximate equation based on the properties of anomalous diffusion and is suitable for gas diffusion in porous media with statistical fractal under steady state, but for unsteady state diffusion in fractal porous media with complex pore structures, new model may be desirable.[10] Thus, the fractional diffusion that is defined as a generalization of diffusion process, which includes non-integer derivatives in the differential equation has drawn more attentions of many researchers.[8,11–13] Zeng and Li

a)Author to whom correspondence should be addressed. Electronic mail: 632851078@qq.com. Tel.: +86 516 83995097. Fax.: +86 516 83995097.

 

(2000)[13] proposed a general form of analytic fractional diffusion equation based on the fractional calculus theory to describe the probability density of particles diffusing on fractal geometry at fractal time and found that the solution connects with the ordinary solutions in the normal space time limit. Jiang and Xu (2006)[14] studied a fractional anomalous diffusion problem caused by an instantaneous point source in disordered fractal media and gave a analytical solutions of concentration distribution. Jiang *et al.* (2010)[15] derived a generalized fractional diffusion model using modified Fick's law and obtained the solution in terms of Mittag-Leffler function using finite Hankel integral transformation and Laplace transformation.

As mentioned above, the fractal diffusion model can reflect the effect of complex pore structure on the transport diffusion process, while the fractional diffusion model allows greater degrees of freedom. An integer order differential operator is a local operator, whereas the fractional order differential operator is non-local; to some extent, it takes into account the fact that a future state does not depends only upon the present state but also upon the history of all its previous states, especially for the porous media that have complex interactions with the gas diffusion in it.

In this work, to study the methane diffusion in coal with adsorption character and highly heterogeneous pore structure,[1,16–20] we established a fractal theory based FFDModel by introducing the fractal dimension $d_f$ to the Fick's classical model and changing the first-order partial differential equation about time into a $\upsilon$ fractional-order partial differential equation. By associating with the given initial and boundary conditions, we try to get the solution of the FFDModel. Furthermore, in order to verify the correctness of the solution, we collected three coal samples from China to do the methane desorption experiment of the fast desorption stage that plays an important role on coal and gas outburst.

## II. ESTABLISHMENT OF THE FFDMODEL

### A. The solution of the FFDModel

Fractional diffusion equations are a useful tool for modeling various anomalous diffusion in complex systems exhibiting pronounced deviations from Fick's classical diffusion model, which is usually described by the following equation:[9]

$$\frac{\partial c(r,t)}{\partial t} = \frac{D}{r^{d-1}}\frac{\partial}{\partial r}\left(r^{d-1}\frac{\partial c(r,t)}{\partial r}\right), \tag{1}$$

where $c$ is the diffusion concentration of the components, (kg/kg); $d$ is the dimension for Euclidean geometry, $D$ is the diffusion coefficient, ($m^2$/s); $r$ is the radius of the coal particles, (m); and $t$ is the time, (s).

Pore structure is one of the major factors that affect the diffusion of methane in coal; The fractal dimension, $d_f$, that can reflect the roughness of pore structure in coal was introduced into Eq. (1) to substitute the Euclidean dimension ($d$) considering the real character of coal. Besides, as described by some researchers,[9,21] the diffusion coefficient $D_e$ in fractal media is not a constant but a function of the position $r$ in the form of $D_e = D_0 r^{-\theta}$, where $D_0$ is the pre-exponential factor, $\theta$ is a structure parameter that can describe the transport path of the diffusing molecule walking randomly in the fractal porous material (for detail in Appendix).

In addition, because of the adsorption character of the coal, the future state of gas diffusion in coal does not only depends upon the present state, but also upon the history of all its previous states, and can be described by a fractional equation, which was obtained by changing the first-order partial differential equation into a $\upsilon$ fractional-order partial differential equation. In general, the range of fractional-order $\upsilon$ is $0 < \upsilon < 2$, in which sub-diffusion corresponds to $0 < \upsilon < 1$, normal diffusion corresponds to $\upsilon = 1$, and super-diffusion corresponds to $1 < \upsilon < 2$.[22] As in fractal porous media, a slowing down phenomenon of gas diffusion due to the irregular path-structure exists, defined as sub-diffusion,[23] in which the fractional-order $\upsilon$ is between 0–1,[24] and in the $0 < \upsilon \le 1$ interval, the diffusion processes exhibit decelerating/acceleration behaviors in long-time range, which is consistent with the diffusion process of methane in coal, thus the interval of $0 < \upsilon \le 1$ is chosen in our study. From the numerical simulation results of Sun *et al.* (2011),[25] we can see that the fractional differential order $\upsilon$ in the fraction equation can reflect the curvature variation of the curve.

Through the substitutions above, the fractal theory based Fractional diffusion model of methane in coal was established[26]

$$\frac{\partial^{\upsilon} c(r,t)}{\partial t^{\upsilon}} = \frac{D_0}{r^{d_f-1}}\frac{\partial}{\partial r}\left(r^{d_f-1-\theta}\frac{\partial c(r,t)}{\partial r}\right), \quad 0 < \upsilon \le 1, \tag{2}$$

where the type of fractional time derivative in this paper is Riemann-Liouville and is defined as $\frac{d^{\upsilon} f(t)}{dt^{\upsilon}} = \frac{d}{dt}\left[\int_0^t \frac{(t-\tau)^{-\upsilon}}{\Gamma(1-\upsilon)} f(\tau)d\tau\right]$,[26,27] $c(r,t)$ is the concentration of diffusion component; for coal particles, at the adsorption equilibrium, the concentration is $c_0$. After the coal particles are exposed to atmospheric conditions, concentration gradients along the radii of the coal particles surface will appear. The adsorbed gas becomes free, and the diffusion from the center of the coal particle to the surface occurs. The surface concentration is $c_1$, and the initial and boundary conditions are as below

$$c(r,t)|_{t=0} = c_0, \quad 0 \le r < r_0, \tag{2a}$$

$$\left.\frac{\partial c(r,t)}{\partial r}\right|_{r=0} = 0, \quad t \ge 0, \tag{2b}$$

$$c(r,t)|_{r=r_0} = c_1, \quad t \ge 0, \tag{2c}$$

where $c_0$ is the initial concentration in an adsorbent, (kg/$m^3$); and $r_0$ is the radius of coal particle, (m).

By performing the transform of $u(r,t) = c(r,t) - c_1$, Eqs. (2) become

$$\frac{\partial^{\upsilon} u(r,t)}{\partial t^{\upsilon}} = \frac{D_0}{r^{d_f-1}}\frac{\partial}{\partial r}\left(r^{d_f-1-\theta}\frac{\partial u(r,t)}{\partial r}\right), \quad 0 < \upsilon \le 1, \tag{3}$$

$$u(r,t)|_{t=0} = c_0 - c_1, \quad 0 \le r < r_0, \tag{3a}$$

$$\left.\frac{\partial u(r,t)}{\partial r}\right|_{r=0} = 0,\ t \geq 0, \tag{3b}$$

$$u(r,t)|_{r=r_0} = 0,\ t \geq 0. \tag{3c}$$

With the transformation of $u(r,t) = T(t)R(r)$ changes Eq. (3) into Eq. (4)

$$\frac{1}{D_0 T(t)} \times \frac{\partial^{\upsilon} T(t)}{\partial t^{\upsilon}} = \frac{1}{r^{\theta}} \times \frac{R''}{R} + \frac{d-1-\theta}{r^{\theta+1}} \times \frac{R'}{R}. \tag{4}$$

By the separation of variables methods: the left side of Eq. (4) becomes a function of $t$, whereas the opposite side becomes a function of $r$; therefore, the two sides of Eq. (4) must be a constant, counted as $-\varepsilon^2$, two types of ordinary differential equations are obtained as follows:

$$T^{\upsilon}(t) + D_0 \varepsilon^2 T(t) = 0, \tag{5}$$

$$\frac{1}{r^{\theta}} \times \frac{R''}{R} + \frac{d-1-\theta}{r^{\theta+1}} \times \frac{R'}{R} = -\varepsilon^2, \tag{6}$$

where $T^{\upsilon}(t) = \frac{\partial^{\upsilon} T(t)}{\partial t^{\upsilon}}$.

Let $x = \frac{2}{d_w} \times r^{\frac{d_w}{2}}$, $R(r) = x^{\alpha} \times f(x)$, where $d_w = 2 + \theta$, $\alpha = \frac{d_w - d_f}{d_w}$, after some calculations, Eq. (6) was changed into a new equation for $f(x)$.

$$x^2 f''(x) + x f'(x) + (\varepsilon^2 x^2 - \alpha^2) f(x) = 0. \tag{7}$$

The general solution of Eq. (7) is

$$f(x) = A J_{\alpha}(\varepsilon x) + B J_{-\alpha}(\varepsilon x), \tag{8}$$

where $A, B$ are random constants, $J_{\alpha}(x)$ is Bessel function with fractional order of $\alpha$.

In that $\alpha < 0$, $\lim_{x \to 0} x^{\alpha} J_{\alpha}(\varepsilon x) = \infty$, and $\forall \alpha$, $\lim_{x \to 0} x^{\alpha} J_{-\alpha}(\varepsilon x) = \frac{(\varepsilon/2)^{-\alpha}}{\Gamma(1-\alpha)}$ (constant), to apply Eq. (8) to all $\alpha$, we should let $A = 0, B = 1$, that is

$$f(x) = J_{-\alpha}(\varepsilon x). \tag{9}$$

From the boundary conditions of (3c), we can obtain $u(r,t)|_{r=r_0} = T(t)R(r_0) = 0$. Because $T(t) \neq 0$, the equation $R(r_0) = 0$ should be satisfied, that is, $R(r_0) = x^{\alpha} f(x_0) = (\frac{2}{d_w} r_0^{\frac{d_w}{2}})^{\alpha} f(\frac{2}{d_w} r_0^{\frac{d_w}{2}}) = 0$. Because $(\frac{2}{d_w} r_0^{\frac{d_w}{2}})^{\alpha} > 0$, Eq. (10) is obtained as follows:

$$f\left(\frac{2}{d_w} r_0^{\frac{d_w}{2}}\right) = 0. \tag{10}$$

By combining Eqs. (9) and (10), Eq. (11) was obtained

$$f\left(\frac{2}{d_w} r_0^{\frac{d_w}{2}}\right) = J_{-\alpha}\left(\varepsilon \times \frac{2}{d_w} r_0^{\frac{d_w}{2}}\right) = 0, \tag{11}$$

where $\varepsilon \times \frac{2}{d_w} r_0^{\frac{d_w}{2}}$ are the roots of $J_{-\alpha}(x)$; supposing that the positive root of the Bessel function $J_{-\alpha}(x)$ is

$$\mu_1 < \mu_2 < \ldots < \mu_n,$$

Then, the Eigen functions are obtained

$$\varepsilon_n{}^2 = \left(\frac{\mu_n d_w}{2 r_0{}^{d_w/2}}\right)^2, \quad n = 1, 2, \ldots. \tag{12}$$

The corresponding eigenfunctions are

$$f_n\left(\frac{2}{d_w} r^{\frac{d_w}{2}}\right) = J_{-\alpha}\left(\mu_n \times \left(\frac{r}{r_0}\right)^{\frac{d_w}{2}}\right), \quad n = 1, 2, \ldots. \tag{13}$$

Take Eq. (13) into $R(r) = x^{\alpha} \times f(x)$,

$$R_n(r) = \left(\frac{2}{d_w}\right)^{\alpha} r^{\frac{d_w - d_f}{2}} J_{-\alpha}\left[\mu_n \left(\frac{r}{r_0}\right)^{\frac{d_w}{2}}\right], \quad n = 1, 2, \ldots. \tag{14}$$

The solution of Eq. (5) is

$$T_n = A_n \times e^{-D_0 \left(\frac{\mu_n d_w}{2 r_0{}^{d_w/2}}\right)^2 t^{\upsilon}}. \tag{15}$$

Because

$$T(t) = \sum_{n=1}^{\infty} T_n(t). \tag{16}$$

Taking Eqs. (14) and (16) into $u(r,t) = T(t)R(r)$

$$u(r,t) = \sum_{n=1}^{\infty} \left(\frac{2}{d_w}\right)^{\alpha} r^{\frac{d_w - d_f}{2}} \times J_{-\alpha}\left[\mu_n \left(\frac{r}{r_0}\right)^{\frac{d_w}{2}}\right] \sum_{n=1}^{\infty} T_n(t), \quad n = 1, 2, \ldots. \tag{17}$$

Applying the boundary conditions (3a) into Eq. (17),

$$\left(\frac{2}{d_w}\right)^{\alpha} r^{\frac{d_w - d_f}{2}} \sum_{n=1}^{\infty} A_n \times J_{-\alpha}\left[\mu_n \left(\frac{r}{r_0}\right)^{\frac{d_w}{2}}\right] = c_0 - c_1. \tag{18}$$

From the orthogonality conditions of Bessel Function, Eq. (19) is obtained

$$\sum_{n=1}^{\infty} A_n = \sum_{n=1}^{\infty} \frac{2(c_0 - c_1)}{\mu_n J_{1-\alpha}(\mu_n)} \times r_0{}^{(d_f - d_w)/2} \times \left(\frac{d_w}{2}\right)^{\alpha}. \tag{19}$$

Take Eq. (19) into Eq. (17),

$$u(r,t) = \sum_{n=1}^{\infty} \frac{2(c_0 - c_1)}{\mu_n J_{1-\alpha}(\mu_n)} \left(\frac{r}{r_0}\right)^{\frac{d_w - d_f}{2}} \times J_{-\alpha}\left[\mu_n \left(\frac{r}{r_0}\right)^{\frac{d_w}{2}}\right] \times e^{-D_0 \left(\frac{\mu_n d_w}{2 r_0{}^{d_w/2}}\right)^2 t^{\nu}}. \tag{20}$$

Therefore,

$$c(r,t) = \sum_{n=1}^{\infty} \frac{2(c_0 - c_1)}{\mu_n J_{1-\alpha}(\mu_n)} \left(\frac{r}{r_0}\right)^{\frac{d_w - d_f}{2}} \times J_{-\alpha}\left[\mu_n \left(\frac{r}{r_0}\right)^{\frac{d_w}{2}}\right] \times e^{-D_0 \left(\frac{\mu_n d_w}{2 r_0{}^{d_w/2}}\right)^2 t^{\nu}} + c_1, \tag{21}$$

$$\frac{c_0 - c(r,t)}{c_0 - c_1} = 1 - \sum_{n=1}^{\infty} \frac{2}{\mu_n J_{1-\alpha}(\mu_n)} \left(\frac{r}{r_0}\right)^{\frac{d_w - d_f}{2}} \times J_{-\alpha}\left[\mu_n \left(\frac{r}{r_0}\right)^{\frac{d_w}{2}}\right] \times e^{-D_0 \left(\frac{\mu_n d_w}{2 r_0^{d_w/2}}\right)^2 t^v}. \quad (22)$$

The cumulative diffusion amount of desorbed methane at time $t$ is expressed in $Q_t$ and the limiting diffusion amount when $t \to \infty$ was expressed as $Q_\infty$

$$\frac{Q_t}{Q_\infty} = \frac{c_0 - \overline{c(r,t)}}{c_0 - c_1} = 1 - \sum_{n=1}^{\infty} \frac{4 d_f}{d_w {\mu_n}^2} e^{-\left(\frac{\mu_n d_w}{2}\right)^2 \frac{D_0}{r_0^{d_w}} t^v}, \quad (23)$$

where

$$\overline{c(r,t)} = \frac{d_f}{{r_0}^{d_f}} \int_0^{r_0} c(r,t) r^{d_f - 1} dr. \quad (24)$$

When the parameters in Eq. (23) change into the following values: $d_f = 3$, $\theta = 0$, correspondingly, $d_w = 2$, $D_0 = D$, $\alpha = -0.5$, $\mu_n = n\pi$, $J_{0.5}\left(\frac{n\pi r}{r_0}\right) = \sqrt{\frac{2 r_0}{n\pi^2 r}} \sin\left(\frac{n\pi r}{r_0}\right)$, $J_{1.5}(n\pi) = \sqrt{\frac{2}{n\pi^2}}(-1)^{n+1}$.

Equations (22) and (23) are transformed into

$$\frac{c_0 - c(r,t)}{c_0 - c_1} = 1 - \frac{2 r_0}{\pi r} \sum_{n=1}^{\infty} \frac{(-1)^{n+1}}{n} \times \sin\left(\frac{n\pi r}{r_0}\right) \cdot e^{-D_0 \left(\frac{n\pi}{r_0}\right)^2 t}, \quad (25)$$

$$\frac{Q_t}{Q_\infty} = 1 - \sum_{n=1}^{\infty} \frac{6}{(n\pi)^2} e^{-(n\pi)^2 \frac{D_0}{r_0^2} t}. \quad (26)$$

This result is consistent with the Fick's classical diffusion model.

### B. Determination of the fractal dimension, $d_f$

In this article, the fractal dimension is determined from an analysis of multilayer adsorption of $N_2$ to a fractal surface according to the FHH (Frenkel-Halsey-Hill) equation

$$\frac{V}{V_0} = K[\ln(P_0/P)]^A, \quad (27)$$

$$A = d_f - 3, \quad (28)$$

where $V/V_0$ is the relative adsorption and $V_0$ and $V$ are the volumes of monolayer coverage and adsorbed gas molecules at equilibrium pressure, respectively, ($m^3$/t). $P_0$ and $P$ are the saturation and equilibrium pressures of the gas, respectively, (MPa), and $K$ is a characteristic constant. $A$ is the power-law exponent that is dependent on $d_f$ and the adsorption mechanism.

Through the logarithmic transformation of Eq. (28), Eq. (29) is obtained

$$\ln\left(\frac{V}{V_0}\right) = \ln \mathrm{K} + (d_f - 3) \ln\left[\ln\left(\frac{P_0}{P}\right)\right]. \quad (29)$$

According to Eq. (28) in the plot of $\ln V$ vs $\ln(\ln(P_0/P))$, the slope ($A$) of the straight-line should be equal to $d_f - 3$. Therefore, the fractal dimension $d_f$ is obtained by $d_f = 3 + A$.

## III. APPLICATIONS OF FFDMODEL IN COAL SAMPLES

### A. Physical property parameters of the coal

Blocks of about 4 kg coal samples with three different metamorphic grade were collected from the working faces of the TieFa, TunLan, and Daning coal mines in China for standard coal analysis, to prevent sample oxidization and moisture loss, all samples were carefully jacketed and then immediately carried to the laboratory for experiments. The measuring results of the maceral and mineral contents, the vitrinite reflectances, the proximate analysis, and part of the $N_2$ adsorption results were shown in Table I.

### B. $N_2$ adsorption/desorption experiment

All coal samples were prepared by sieving to a maximum size of 3 mm and were dried at 473 K for 24 h in a vacuum oven. After drying, samples were sieved again to obtain the same particle size fraction of 0.2–0.25 mm. Outgassing and determination of adsorption isotherms were carried out using an Autosorb-1 (Quanta-chrome Instrument Corporation). The samples were initially outgassed at 473 K overnight under vacuum to a final pressure of 0.25 Pa before adsorption isotherms were generated by dosing nitrogen at 77 K on the samples. The BET specific surface area, pore volume, average pore diameter, and pore size distributions were obtained from these measurements. The relative pressure ($P/P_0$) ranged from 0.001 to 0.99.

In this article, the adsorption isotherm data ($P_0/P, V$) of $N_2$ are obtained according to the method described in Sec. II B. Based on the adsorption isotherm data, the fractal dimension ($d_f$) is obtained using Eq. (29). Figs. 1(a)–1(c) shows the FHH plots of the three coal samples.

TABLE I. Basic physical property parameters of the coal samples.

| | | Maceral and mineral (vol. %) | | | | | Proximate analysis/% | | | | | |
|---|---|---|---|---|---|---|---|---|---|---|---|---|
| Coal mine | Coal type | Vitrinite | Intertinite | Liptinite | Mineral | Vitrinite reflectance | $M_{ad}$ | $A_d$ | $V_{daf}$ | $FC_d$ | Average pore diameter/Å | Multipoint BET/($m^2$/g) |
| TieFa | Long flame coal | 91.60 | 5.50 | 0 | 2.9 | 0.6038 | 6.77 | 19.745 | 38.77 | 49.14 | 75.25 | 4.794 |
| TunLan | Coking coal | 88.65 | 2.3 | 0 | 9.05 | 1.85 | 0.89 | 22.89 | 19.63 | 61.99 | 220.2 | 0.5375 |
| DaNing | Anthracite | 77.8 | 14.1 | 0 | 8.1 | 3.6 | 3.46 | 25.63 | 8.61 | 68.05 | 36.01 | 43.77 |

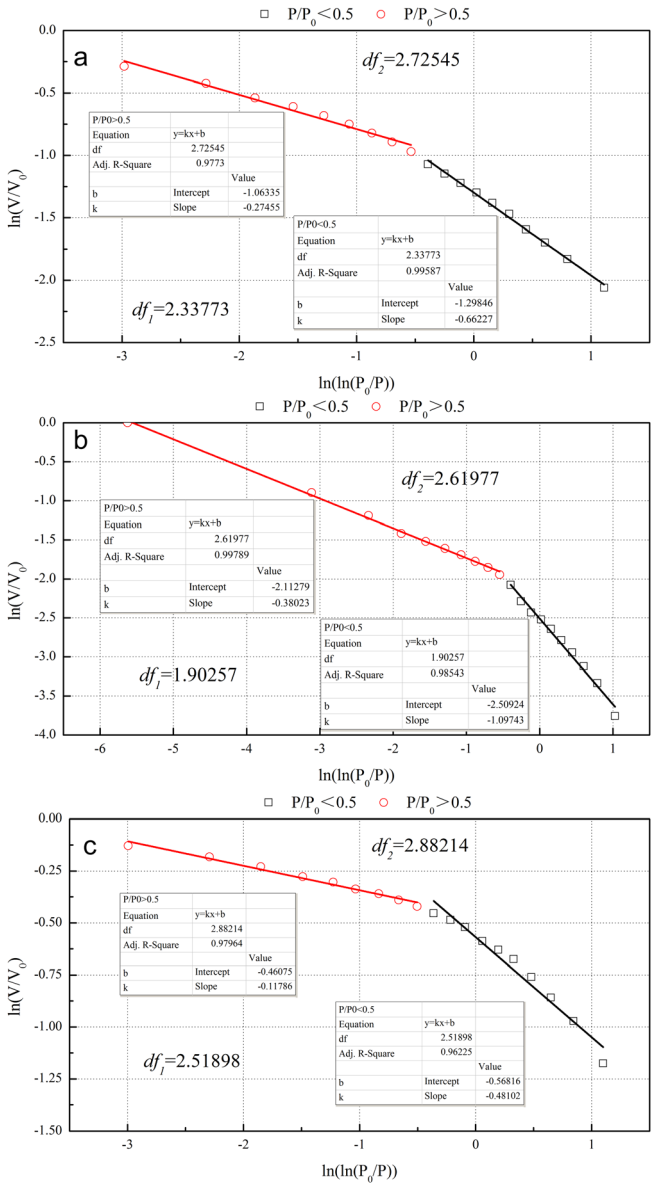


FIG. 1. Plots of $\ln V$ vs $\ln(\ln(P_0/P))$ reconstructed from the $N_2$ adsorption/desorption isotherms of the three coal samples (a: Long flame coal; b: coking coal; and c: anthracite).

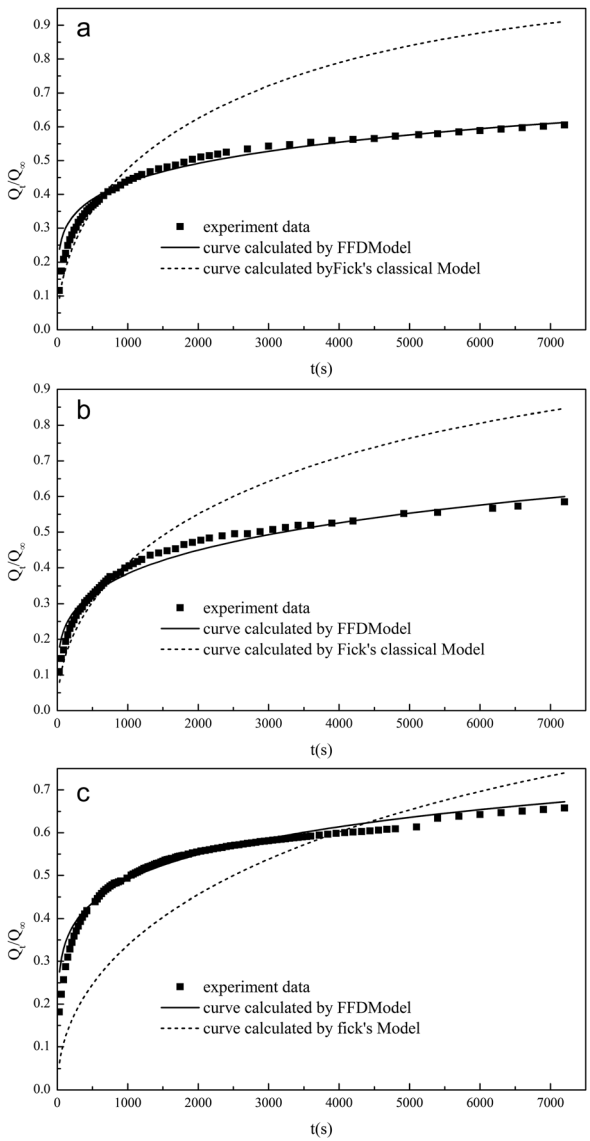


FIG. 2. The fast desorption curve of the three coal samples from China (a: Long flame coal; b: coking coal; and c: anthracite).

From Figs. 1(a)–1(c), we can see that there are two distinct linear segments over the relative pressure ($P/P_0$) range of 0–0.5 and 0.5–1. Both of these segments show good fits. As described in Eq. (29), the fractal dimension value ($d_{f1}$ and $d_{f2}$) were calculated from the slope of the two linear segments, Table II shows the calculation results the slopes of regression lines ($A_1$ and $A_2$) and fractal dimension values ($d_{f1}$ and $d_{f2}$) calculated at the relative pressure ($P/P_0$) interval of 0–0.5 and 0.5–1.

From Table II, we can see that both $d_{f1}$ and $d_{f2}$ initially increase and then decrease with the metamorphic grade of coal and the variation of $d_{f1}$ in the lower 0.5–1 relative pressure interval are smaller than $d_{f2}$. $d_{f1}$ are ranging from 1.90257 to 2.51898, while the $d_{f2}$ is from 2.61977 to 2.88214, both of the value of $d_{f1}$ and $d_{f2}$ in coking coal are the lowest of the three coal types; This result is consistent with the specific surface of the coal samples.

TABLE II. Fractal dimensions derived from fractal FHH model.

| | | $P/P_0 < 0.5$ | | | $P/P_0 > 0.5$ | | |
|---|---|---|---|---|---|---|---|
| Coal mine | Coal type | $A_1$ | $d_{f1}$ | $\hat{R}_1$ | $A_2$ | $d_{f2}$ | $\hat{R}_2$ |
| TieFa | Long flame coal | −0.66227 | 2.33773 | 0.99587 | −0.27455 | 2.72545 | 0.9773 |
| TunLan | Coking coal | −1.09743 | 1.90257 | 0.98543 | −0.38023 | 2.61977 | 0.99789 |
| DaNing | anthracite | −0.48102 | 2.51898 | 0.96225 | −0.11786 | 2.88214 | 0.97964 |

TABLE III. Results from the comparison of the FFDModel and Fick's classical model.

| | | | | | | | correlation factor in Fick's classical model | | correlation factor in FFDModel | |
|---|---|---|---|---|---|---|---|---|---|---|
| Coal mine | Coal type | $\upsilon$ | $D_F/(m^2/s)$ | $\theta$ | $D_0$ | $D_e$ | $\hat{R}_{1F}$ | $\hat{R}_{2F}$ | $\hat{R}_{1FFDM}$ | $\hat{R}_{2FFDM}$ |
| TieFa | Long flame coal | 0.415 | 3.382E-13 | 1.891 | 4.84E-19 | 1.4066E-11 | 0.976 | 0.756 | 0.987 | 0.949 |
| TunLan | Coking coal | 0.54 | 2.426E-13 | 1.751 | 5.70E-19 | 4.638E-12 | 0.977 | 0.824 | 0.987 | 0.956 |
| DaNing | anthracite | 0.39 | 3.526E-13 | 1.855 | 9.80E-19 | 2.072E-11 | 0.961 | 0.798 | 0.982 | 0.976 |

### C. Desorption experiments

The core sampling method was used to prepare the coal samples for the standard desorption tests. The collected coal samples were crushed into particles of $0.2 \sim 0.25$ mm using a sampling machine. The gas used for the desorption tests was CH4 with a purity of about 99.99%, and the experiments were conducted in a FM4WP-1 desorption instrument.

For the adsorption isotherm of $N_2$ in coal samples, in the section of $P/P_0 > 0.5$, the surface of the coals were all covered by $N_2$ molecules, so the adsorption isotherm data after $P/P_0 = 0.5$ are used to calculate in the FFDModel. By substituting $d_{f2}$ into Eq. (23) and applying the positive zero of the Bessel function and by fitting the FFDModel with the experimental data, the parameters $\nu$ (reflecting the variation trend of the desorption curve[25]) and $\theta$ (presenting the transport path) were obtained. The calculating results from the FFDModel and Fick's classical model for comparison with experimental data are shown in Figs. 2(a)–2(c).

From Figs. 2(a)–2(c), we can see that the change law of the relative desorption curve is basically the same, i.e., the desorption speed is initially fast. The influence of the microstructure mesh is obvious along with the diffusion time, and the difference between the FFDModel and Fick's classical model is obvious. The channel is regular when the $d_f'\theta$ are small, and the calculated relative adsorption amounts are also small.

We can also see from Figs. 2(a)–2(c) that at the initial time, the relative adsorption curve for the FFDModel is higher than Fick's classical model because at the initial time, the influence of the structure parameter $\theta$ that represent the transport path is not obvious but the fractal dimension $d_f$ is smaller than in Fick's classical model. With increased time, the influence of the structure parameter $\theta$ is obvious, but there is no structure parameter $\theta$ in Fick's classical model; therefore, Fick's classical model cannot describe the transport path of gas in the porous coal; and consequently, the growth rate of the relative adsorption curve of Fick's classical model is faster than the FFDModel. Therefore, we can see that the relative adsorption curve in the FFDModel intersects with Fick's classical model. And it is clear that qualitative differences observed in the desorption data calculated by FFDModel could be considered having no differences with the experimental data because of the high contact ratio. From a point of quantitative view, we defined two correlation factor $\hat{R}_1$ and $\hat{R}_2$

$$\hat{R}_1 = \frac{\sum((Q_t/Q_\infty)_{cal} - \overline{(Q_t/Q_\infty)_{cal}})((Q_t/Q_\infty)_{\exp} - \overline{(Q_t/Q_\infty)_{\exp}})}{\sqrt{\sum((Q_t/Q_\infty)_{cal} - \overline{(Q_t/Q_\infty)_{cal}})^2 \times \sum((Q_t/Q_\infty)_{\exp} - \overline{(Q_t/Q_\infty)_{\exp}})^2}}, \tag{30}$$

$$\hat{R}_2 = 1 - \frac{\sum|(Q_t/Q_\infty)_{cal} - (Q_t/Q_\infty)_{\exp}|}{\sum(Q_t/Q_\infty)_{\exp}}. \tag{31}$$

The fitting results of the two models were shown in Table III.

From Table III, we can see that the magnitudes of the diffusivity $D_e$ in the FFDModel are between $10^{-11} \sim 10^{-12}$. The magnitudes of the pre-exponential coefficient $D_0$ are between$10^{-20} \sim 10^{-19}$. The magnitudes of the diffusivity $D_F$ in the Fick's classical model are about $10^{-13}$. The diffusivity in both of the FFDModel and Fick's classical model first decreases then increases with the coal metamorphic grade. The structure parameter $\theta$ reflecting the transport path has the same changing law with the diffusivity, and the fractional order $\nu$ has the inverse law with the diffusivity. Moreover, the degree of fitting the FFDModel is higher than that of Fick's classical model. In other words, for the fast desorption stage of methane in coal, the FFDModel fits better.

## IV. CONCLUSIONS

(1) The fractal dimension $d_{f1}$ and $d_{f2}$ which reflect the surface roughness of coal initially decrease and then increase with the metamorphic grade of coal and the value of $d_{f1}$ and $d_{f2}$ in coking coal are the lowest of the three coal types. This result is consistent with the specific surface of coal samples.

(2) The magnitudes of the diffusivity $D_e$ in the FFDModel are between $10^{-11}$ and $10^{-12}$. The magnitudes of the

pre-exponential coefficient $D_0$ are between$10^{-20}$ and $10^{-19}$. The magnitudes of the diffusivity $D_F$ in the Fick's classical model are about $10^{-13}$. The diffusivity in both of the FFDModel and Fick's classical model first decreases and then increases with the coal metamorphic grade. The structure parameter $\theta$ which reflect the transport path has the same changing law with the diffusivity, and the fractional order $\nu$ which reflect the curvature of the desorption curve has the inverse law with the diffusivity.

(3) The fitting degree of the FFDModel is higher than the Fick's classical model. Furthermore, FFDModel fits better with the fast desorption stage of methane in coal.

## NOMENCLATURE

FFDModel A fractal theory based Fractional diffusion model

$c$ = the diffusion concentration of the components
$c_0$ = the concentration at the adsorption equilibrium
$c_1$ = the surface concentration
$d$ = the dimension for Euclidean geometry
$d_f$ = fractal dimension
$D$ = diffusivity
$D_0$ = pre-exponential coefficient
$\theta$ = structure parameter that reflect the transport path of methane in coal
$P_0$ = the saturation pressures
$P$ = the equilibrium pressures
$r$ = the radius of the coal particles
$t$ = time
$\upsilon$ = fractional order of FFDModel that reflect the curvature of the desorption curve
$V/V_0$ = the relative adsorption
$V_0$ = the volumes of monolayer coverage
$V$ = the volume of adsorbed gas molecules at equilibrium pressure

## ACKNOWLEDGMENTS

This research was supported by the Fundamental Research Funds for the Central Universities (No. 2012LWB02), and we appreciate the editors and anonymous reviewers for their valuable comments.

## APPENDIX: DIFFUSION LAW IN FRACTAL MEDIA

In homogeneous and isotropic media, a diffusing substrate molecule is performing a random walk through a medium without any disorder, i.e., all of step in the diffusion process have equal length and travel time,[28] the mean-square displacement, $\langle r^2(t)\rangle$, grows proportional to the time. This is called a normal diffusion law and usually is denoted as: $\langle r^2(t)\rangle \propto t$ or equivalently $\langle r^2(t)\rangle = D_F t$; where $D_F$ is the diffusion coefficient.[8,29]

In nature, many porous media exhibit a fractal pore structure that can be described by fractal theory[19,30–34] in which the fractal dimension $d_f$ is an effectual parameter that can reflect the roughness of the pore structure. In fractal media, the diffusing molecule is not able to access to every place throughout it, which is the length of steps in the diffusion process are not equal,[28] the mean-square displacement $\langle r^2(t)\rangle$ in the media has a power law function of time, this is called "anomalous diffusion"[29] and is denoted in the form of $\langle r^2(t)\rangle \propto t^{\frac{2}{d_w}}$, where $d_w > 2$ is the anomalous diffusion exponent.[7,8,11,13,35] Some other researchers[36] define $d_w$ as "statistical fractal dimension" of the diffusion process. The above scaling relationship provides a means to categorize different diffusion processes. For "normal" diffusion, $d_w$ is exactly 2, which leads to the linear dependence of $\langle r^2(t)\rangle$ on diffusion-time mentioned above. When the mean-squared displacements increase more rapidly, i.e., $d_w < 2$, the process is considered to be in the super diffusive regime. The opposite case of $d_w > 2$ is encountered in a sub diffusion process.[36–38] Because of the irregular path-structure of a fractal porous media, a slowing down phenomenon of gas diffusion happened during the transport diffusion process, which belongs to sub diffusion.

On a fractal object, the effective diffusion coefficient $D_e$ depends upon time or space according to the following laws: $D_e \propto \frac{\langle r^2(t)\rangle}{t}$. By combining the equation $\langle r^2(t)\rangle \propto t^{\frac{2}{d_w}}$, we have $D_e \propto \langle r^2(t)\rangle^{\frac{-\theta}{2}}$ by eliminating the variable $t$, where $\theta = d_w - 2$, $\theta$ is a structure parameter that describes the transport path of the diffusing molecule walking randomly in the fractal porous material,[7,36] by assuming the mean-square displacement in the random walk equal to the $r$ that represents the distance to an arbitrary origin, then we have $D_e \propto r^{-\theta}$, which is consistent with the result of O'Shaughnessy and Procaccia (1985),[6] Randriamahazaka *et al.* (2002),[7] and the equation $D_e \propto r^{-\theta}$ means that the effective diffusion coefficient $D_e$ in fractal media is not a constant but a function of the position $r$ in the form of $D = D_0 r^{-\theta}$, where $D_0$ is the pre-exponential factor.

[1]M. Pillalamarry, S. Harpalani, and S. Liu, Int. J. Coal Geol. **86**(4), 342 (2011).
[2]A. Marecka and A. Mianowski, Fuel **77**(14), 1691 (1998).
[3]B. Bijeljic, S. Rubin, H. Scher, and B. Berkowitz, J. Contam. Hydrol. **120–121**(0), 213 (2011).
[4]G. Srinivasan, D. M. Tartakovsky, M. Dentz, H. Viswanathan, B. Berkowitz, and B. A. Robinson, J. Comput. Phys. **229**(11), 4304 (2010).
[5]T. Le Borgne, M. Dentz, D. Bolster, J. Carrera, J. de Dreuzy, and P. Davy, Adv. Water Resources **33**(12), 1468 (2010).
[6]B. O'Shaughnessy and I. Procaccia, Phys. Rev. Lett. **54**, 455 (1985).
[7]H. Randriamahazaka, V. Noël and C. Chevrot, J. Electroanal. Chem. **521**(1–2), 107 (2002).
[8]M. Giona and H. Eduardo Roman, Physica A **185**(1–4), 87 (1992).
[9]S. Wang, Z. Ma, and H. Yao, Chem. Eng. Sci. **64**(6), 1318 (2009).
[10]Q. Zheng, B. Yu, S. Wang, and L. Luo, Chem. Eng. Sci. **68**(1), 650 (2012).
[11]Q. Zeng, H. Li and D. Liu, Commun. Nonlinear Sci. Numer. Simul. **4**(2), 99 (1999).
[12]J. R. Leith, Signal Process. **83**(11), 2397 (2003).
[13]Q. H. Zeng and H. Q. Li, Fractals **8**(1), 117 (2000).
[14]J. Xiaoyun and X. M. Yu, Int. J. Non-Linear Mech. **41**(1), 156 (2006).
[15]X. Jiang, M. Xu, and H. Qi, Nonlinear Anal.: Real World Appl. **11**(1), 262 (2010).
[16]A. Saghafi, M. Faiz, and D. Roberts, Int. J. Coal Geol. **70**(1–3), 240 (2007).
[17]N. Siemons, K. A. A. Wolf, and J. Bruining, Int. J. Coal Geol. **72**(3–4), 315 (2007).

[18]J. Yi, I. Y. Akkutlu, C. Ö. Karacan, and C. R. Clarkson, Int. J. Coal Geol. **77**(1–2), 137 (2009).
[19]Y. Cai, D. Liu, Z. Pan, Y. Yao, J. Li, and Y. Qiu, Fuel **103**(0), 258 (2013).
[20]X. Cui, R. M. Bustin, and G. Dipple, Fuel **83**(3), 293 (2004).
[21]D. H. Zhang, S. M. Heng, J. Feng, and Y. Hao, J. Eng. Thermophys. **25**(5), 822 (2004) (in Chinese).
[22]R. Metzler and J. Klafter, Europhys. Lett. **51**(5), 492 (2000).
[23]C. Marguerit, D. Schertzer, F. Schmitt, and S. Lovejoy, J. Marine Syst. **16**(1–2), 69 (1998).
[24]G. Fernandez-Anaya, F. J. Valdes-Parada, and J. Alvarez-Ramirez, Physica A **390**(23–24), 4198 (2011).
[25]H. Sun, Y. Chen, and W. Chen, Signal Process. **91**(3), 525 (2011).
[26]R. Metzler, W. G. Glöckle, and T. F. Nonnenmacher, Physica A **211**(1), 13 (1994).
[27]N. Heymans and I. Podlubny, Rheol. Acta **45**(5), 765 (2006).
[28]A. Sharifi-Viand, M. G. Mahjani, and M. Jafarian, J. Electroanal. Chem. **671**(0), 51 (2012).
[29]I. Hironobu, I. Shinichi, and M. A. Adams, Phys. B: Condens. Matter **241**(0), 585 (1997).
[30]W. I. Friesen and R. J. Mikula, J. Colloid Interface Sci. **120**(1), 263 (1987).
[31]L. Xu, D. Zhang, and X. Xian, J. Colloid Interface Sci. **190**(2), 357 (1997).
[32]Y. Yao, D. Liu, D. Tang, S. Tang, and W. Huang, Int. J. Coal Geol. **73**(1), 27 (2008).
[33]Y. Yao, D. Liu, D. Tang, S. Tang, W. Huang, Z. Liu, and Y. Che, Comput. Geosci. **35**(6), 1159 (2009).
[34]C. Wang, S. Hao, W. Sun, and W. Chu, Int. J. Mining Sci. Technol. **22**(6), 855 (2012).
[35]F. Ren, J. Liang, W. Qiu, X. Wang, Y. Xu, and R. R. Nigmatullin, Phys. Lett. A **312**(3–4), 187 (2003).
[36]E. Özarslan, T. M. Shepherd, C. G. Koay, S. J. Blackband, and P. J. Basser, NeuroImage **60**(2), 1380 (2012).
[37]C. Li, W. Deng, and Y. Wu, Comput. Math. Appl. **62**(3), 1024 (2011).
[38]R. Metzler and J. Klafter, Phys. Rep. **339**(1), 1 (2000).